Geometry-induced motion of magnetic domain walls in curved nanostripes

Kostiantyn V. Yershov,[1,2,*] Volodymyr P. Kravchuk,[1,3,†] Denis D. Sheka,[4,‡] Oleksandr V. Pylypovskyi,[4,§]
Denys Makarov,[5,‖] and Yuri Gaididei[1,¶]

[1]*Bogolyubov Institute for Theoretical Physics of the National Academy of Sciences of Ukraine, 03143 Kyiv, Ukraine*
[2]*National University of Kyiv-Mohyla Academy, 04655 Kyiv, Ukraine*
[3]*Leibniz-Institut für Festkörper- und Werkstoffforschung, IFW Dresden, Dresden D-01171, Germany*
[4]*Taras Shevchenko National University of Kyiv, 01601 Kyiv, Ukraine*
[5]*Helmholtz-Zentrum Dresden-Rossendorf e.V., Institute of Ion Beam Physics and Materials Research, 01328 Dresden, Germany*

Dynamics of topological magnetic textures are typically induced externally by, e.g., magnetic fields or spin/charge currents. Here, we demonstrate the effect of the internal-to-the-system geometry-induced motion of a domain wall in a curved nanostripe. Being driven by a gradient of the curvature of a stripe with biaxial anisotropy, transversal domain walls acquire remarkably high velocities of up to 100 m/s and do not exhibit any Walker-type speed limit. We pinpoint that the inhomogeneous distribution of the curvature-induced Dzyaloshinskii-Moriya interaction is a driving force for the motion of a domain wall. Although we showcase our approach on the specific Euler spiral geometry, the approach is general and can be applied to a wide class of geometries.

The deterministic manipulation of magnetic textures, e.g., domain walls (DWs) and skyrmions, in magnetic stripes is a key practical task to realize high-speed, high-density, low-power, and nonvolatile memory devices [1–4]. Typically, the motion of DWs is realized externally by applying a magnetic field [5–7] or electric current [8–10], including curvilinear geometries [11,12]. The main hurdle on the way toward achieving high translational speed for DWs is the appearance of the Walker limit [13–15], which imposes a maximum value of the driving force (magnetic field, current density) for translational motion. Several approaches have been proposed to achieve a high-speed translational DW motion: usage of antiferromagnetically coupled magnetic nanowires [16,17], application of spin currents perpendicular to the wire [18], and application of spin-orbit torques for chiral DWs [19,20]. In spite of the fact that maximum value of the driving force is zero for the case of head-to-head (tail-to-tail) DWs in wires with uniaxial anisotropy, one can realize DW motion with a high and constant velocity in the precessional regime with a uniform rotation of the DW phase [21]. Furthermore, it was shown that the curvature has a drastic influence on the Walker limit [22–27]. For example, under certain conditions, the Walker limit can be suppressed in nanotubes [26,27]. An alternative way to achieve the motion of DWs is based on the deformation of the DW structure and known as automotion [28–31]. This type of motion can be realized relying on the coordinate-dependent cross-sectional area of a nanostripe [30,31],

nucleation of DWs with inertial motion [29], or transformation of DWs from the transversal to the vortex [28] by short current pulses.

Here, we propose a concept of geometry-induced motion of topological defects in a curved nanostripe. We demonstrate that a DW performs a translational motion under the influence of the gradient of the stripe curvature. As we do not observe a transition to the precessional regime of motion in the case of a biaxial as well as uniaxial anisotropy, the geometry-induced motion is free of a Walker-type speed limit. We pinpoint that the inhomogeneous distribution of the curvature-induced Dzyaloshinskii-Moriya interaction (DMI) driven by the exchange [32,33] acts as a driving force for the motion of transversal DWs in curved nanostrips. We propose a general approach valid for a wide class of geometries. The analytical results are confirmed by means of micromagnetic simulations.

We consider a flat narrow curved ferromagnetic stripe of a rectangular cross section whose thickness and width are small enough to ensure the magnetization uniformity along a wire cross section. The stripe length is substantially larger than the transversal dimensions. Thus, the magnetization is described by the continuous and normalized function $\boldsymbol{m} = \boldsymbol{M}/M_s = \boldsymbol{m}(s,t)$, where M_s is the saturation magnetization, s is the arc length coordinate, and t denotes time. Such a stripe can be parametrized in the following way: $\boldsymbol{r}(s,\xi_1,\xi_2) = \boldsymbol{\gamma}(s) + \xi_1 \boldsymbol{e}_{\mathrm{N}}(s) + \xi_2 \boldsymbol{e}_{\mathrm{B}}(s)$. Here, the three-dimensional radius vector $\boldsymbol{r}$ defines the space domain, occupied by the stripe, $\boldsymbol{\gamma}(s) = \gamma_x(s)\hat{\boldsymbol{x}} + \gamma_y(s)\hat{\boldsymbol{y}}$ is a two-dimensional vector, which lies within the xy plane and determines the stripe center line (see Fig. 1). The parameters $\xi_1 \in [-w/2, w/2]$ and $\xi_2 \in [-h/2, h/2]$ are coordinates in the transversal cross section $w \geqslant h$ (see Fig. 1).

The magnetic properties of a narrow ferromagnetic stripe are described using a model of a classical ferromagnetic wire with a biaxial anisotropy. The easy axis is tangential to the

─────────

*Corresponding author: yershov@bitp.kiev.ua

†vkravchuk@bitp.kiev.ua

‡sheka@knu.ua

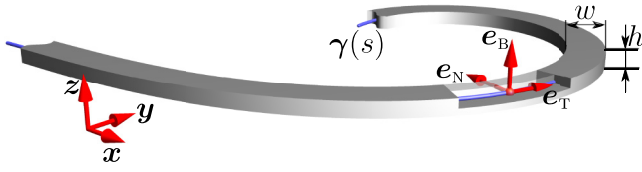§engraver@knu.ua

‖d.makarov@hzdr.de

¶ybg@bitp.kiev.ua

FIG. 1. Geometry and notations: we consider a one-dimensional curved ferromagnet of thickness h and width w with the easy axis e_T and easy plane TN anisotropies.
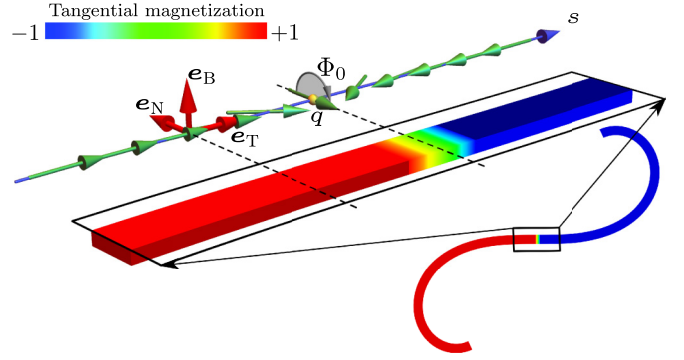

FIG. 2. Illustration of a one-dimensional head-to-head DW ($p = +1$ and $C = -1$) geometry in a stripe with the shape of an Euler spiral described by two collective coordinates: the DW position q and phase Φ. Red axes determine curvilinear basis; green arrows and color scheme determine the magnetization distribution in the stripe obtained by means of NMAG micromagnetic simulations. Simulation is performed for the Permalloy stripe with $h = 5$ nm, $w = 15$ nm, and $\chi \ell^2 = 2 \times 10^{-4}$ in an overdamped regime ($\alpha = 0.5$).

stripe central line γ, whereas the easy plane coincides with the stripe plane (TN plane). The magnetic energy of the stripe normalized by $4\pi M_s^2$ reads

$$\mathcal{E} = \mathcal{S} \int_{-\infty}^{\infty} \{ \mathscr{E}_{ex} + k_a [1 - (m \cdot e_T)^2] + k_p (m \cdot e_B)^2 \} ds. \tag{1}$$

Here, $\mathcal{S} = hw$ is the cross-section area. The first term in (1) is the exchange energy density $\mathscr{E}_{ex} = \ell^2 \sum_{i=x,y,z} (\partial_i m)^2$ with $\ell = \sqrt{A/(4\pi M_s^2)}$ being the exchange length where A is the exchange constant. The last two terms in (1) determine the anisotropy energy density. Vectors e_T and e_B are unit vectors along the anisotropy axes, which are assumed to be oriented along the tangential and binormal directions [34]. Constants $k_a = K_a/(4\pi M_s^2) + k_a^{ms}$ and $k_p = K_p/(4\pi M_s^2) + k_p^{ms}$ are dimensionless anisotropy constants of easy-tangential and easy-plane types, respectively, with $K_a > 0$ and $K_p > 0$ being magnetocrystalline anisotropy constants. Terms k_a^{ms} and k_p^{ms} arise from the magnetostatic contribution. It is known [7,35,36] that the magnetostatic energy of a straight and uniformly magnetized stripe with rectangular cross section can be reduced to the effective shape anisotropy [36] with constants

$$k_a^{ms} = \frac{\frac{1-\delta^2}{2\delta} \ln(1 + \delta^2) + \delta \ln \delta + 2 \arctan \frac{1}{\delta}}{2\pi},$$

$$k_p^{ms} = \frac{1}{2} - 2k_a^{ms}, \quad \delta = w/h \geqslant 1. \tag{2}$$

For thin, narrow, and curved stripes (ribbons) the approximation of the shape anisotropy is used also for inhomogeneous magnetization states [37], including domain walls [15]. In the limit case of square ($w/h = 1$) or circular cross sections, the magnetostatic-shape-induced anisotropy coefficients (2) are simplified to $k_a^{ms} = 1/4$ and $k_p^{ms} = 0$, which is a well-known result [7,38] including the case of curvilinear wires [39].

The energy density (1) in terms of the angular parametrization $m = e_T \cos\theta + e_N \sin\theta \cos\phi + e_B \sin\theta \sin\phi$ has the following form:

$$\mathscr{E} = \ell^2 [(\theta' + \kappa \cos\phi)^2 + (\phi' \sin\theta - \kappa \cos\theta \sin\phi)^2]$$
$$+ \sin^2 \theta (k_a + k_p \sin^2 \phi), \tag{3}$$

where the first term corresponds to the exchange energy density in the curved wire [33] with κ being a curvature of the γ. In (3) it is taken into account that a flat wire has zero torsion.

To analyze the dynamics of a DW in a curved magnetic stripe we use a collective variable approach based on the $q - \Phi$ model [5,40]

$$\cos\theta = -p \tanh \frac{s - q}{\Delta}, \quad \phi = \Phi. \tag{4}$$

Here, $\{q, \Phi\}$ are time-dependent conjugated collective variables, which determine the DW position and phase, respectively (see Fig. 2); Δ is a DW width; p is a topological charge, which determines the DW type: head-to-head ($p = +1$) or tail-to-tail ($p = -1$). The model (4) coincides with the exact DW solution for a rectilinear wire ($\kappa' \equiv 0$). In the following, the curvature is considered as a small perturbation, which results in the DW drift while keeping the form (4) unchanged. The analysis is carried out in the approximation linear with respect to the curvature and its gradient: $\kappa \ell / \sqrt{k_a} \ll 1$ and $\kappa' \ell^2 / k_a \ll 1$.

Substituting the ansatz (4) into (3) and performing integration over the arc length s, we obtain the energy of a DW in a curved stripe in the form (up to an additive constant and quadratic terms with respect to κ)

$$\frac{\mathcal{E}}{2\mathcal{S}} \approx \frac{\ell^2}{\Delta} + \Delta k_a + \Delta k_p \sin^2 \Phi + p\pi \kappa(q) \ell^2 \cos\Phi, \tag{5}$$

where the condition $\kappa \Delta \ll 1$ was applied when integrating (3). The first three terms in (5) determine the competition of the isotropic exchange and anisotropy contributions, while the forth term originates from the curvilinear-geometry-induced DMI driven by the exchange [32,33]. The last term in the energy (5) demonstrates the coupling between the curvature, DW topological charge, and phase, i.e., exchange energy is minimized when $\cos\Phi = -\text{sgn}(p\kappa)$. This allows the following geometrical interpretation: the averaged nonuniformity of the DW magnetization structure can be controlled by the DW wall phase Φ if the curvature is present (see Fig. 1 in Ref. [41]).

In terms of the collective variables, the equations of motion take a form [42]

$$\frac{\alpha}{\Delta} \dot{q} + p\dot{\Phi} = -p\pi \omega_0 \ell^2 \frac{\partial \kappa(q)}{\partial q} \cos\Phi,$$

$$p\dot{q} - \alpha\Delta\dot{\Phi} = -p\pi \omega_0 \ell^2 \kappa(q) \sin\Phi + k_p \Delta\omega_0 \sin 2\Phi, \tag{6}$$

where α is the damping parameter, and $\omega_0 = 4\pi \gamma_0 M_s$ determines the characteristic timescale of the system with
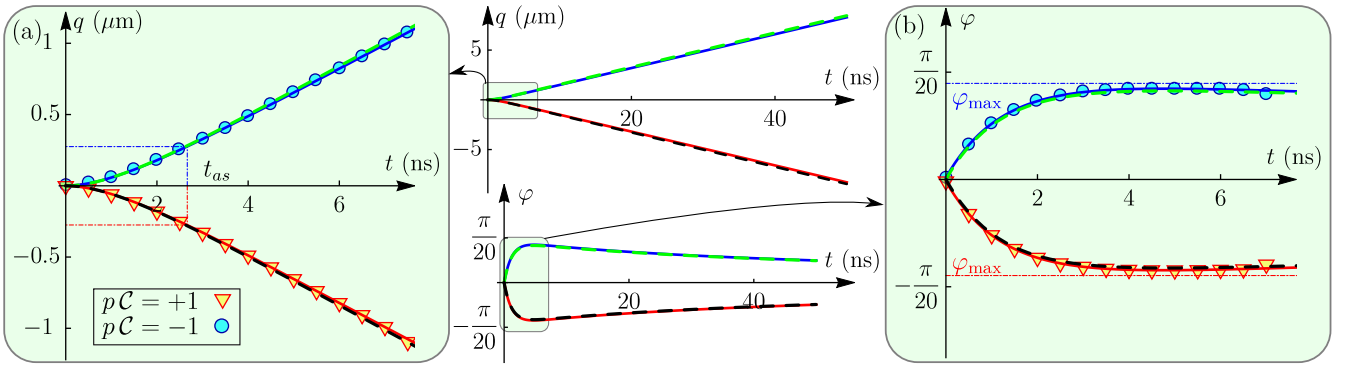
FIG. 3. Typical behavior of the DW position (a) and phase deviation (b) for a head-to-head DW ($p = +1$). Geometrical parameters of the stripe are as follows: $\chi \ell^2 = 2 \times 10^{-4}$, $w = 15$ nm, $h = 5$ nm. Solid and dashed lines correspond to solutions of the collective variables equations (6) and predictions of the linearized model [42], respectively. Asymptotic time calculated accordingly to (9) for $\varepsilon = 0.9$. Symbols show the results of NMAG micromagnetic simulations. Central inset demonstrates the comparison of solutions of the collective variables equations (6) and predictions of the linearized model of long-time dynamics. In all cases $\alpha = 0.01$ and $K_a = K_p = 0$.

γ_0 being the gyromagnetic ratio. The DW width is assumed to be a slaved variable [7,22], i.e., $\Delta(t) \equiv \Delta[\Phi(t)] = \ell / \sqrt{k_a + k_p \sin^2 \Phi}$. The behavior of the DW width is discussed in detail in the Supplementaly Material [42]. From (6) it follows that the gradient of the curvature is a driving force for DWs. The physical origin of this force is the curvilinear-geometry-induced DMI driven by the exchange.

The ground state in a curved wire ($\kappa' \neq 0$) cannot be strictly tangential: the magnetization vector $\boldsymbol{m}$ deviates from the tangential direction by an angle $\vartheta \approx \chi \ell^2 / k_a$ (for the case $\kappa' \equiv \chi$) in the TN plane. This effect results in the modification of Eqs. (6) up to corrections in curvature and its gradient of the second order of magnitude [42]. Therefore, the carried out analysis of the DW motion in the approximation linear with respect to the curvature and its gradient is valid.

In the following we apply the general $q - \Phi$ equations of motion (6) for a particular case of an Euler spiral [43], also known as Cornu spiral or clothoid (see Fig. 2). The equation for the central line of such a stripe has the form

$$\boldsymbol{\gamma}(s) = \hat{x} \int_0^s \cos\left(\frac{\chi}{2}\zeta^2\right) d\zeta + \hat{y} \int_0^s \sin\left(\frac{\chi}{2}\zeta^2\right) d\zeta. \quad (7)$$

The curvature in this case is a linear function of the arc length coordinate $\kappa(s) = \chi s$ with χ being the gradient of the curvature. It is necessary to mention that we are interested in the stripes of a finite width w. Therefore, to avoid an overlap between the neighboring windings of the spiral, the distance between them must be bigger than the stripe width w. The minimal distance between windings is determined by the condition $\kappa w \ll 1$.

Using a small-angle approximation for the DW phase $\varphi = \Phi - \Phi_0 \ll 1$ [44], we obtain the asymptotic expression for the wall velocity [42]

$$V = -p\, \mathcal{C} \pi \, \Delta_0 \omega_0 \frac{\chi \ell^2}{\alpha}, \quad (8)$$

where $\mathcal{C} = \cos \Phi_0 = \pm 1$ with Φ_0 being the initial DW phase, $\Delta_0 = \ell / \sqrt{k_a}$. In the following it will be shown that the initial value of the DW phase coincides with $\Phi(t \to \infty)$. Therefore, we can interpret $\mathcal{C}$ as the DW magnetochirality [45]. For a curved nanowire [46–48] with the curvature $\kappa \in$

$[0; 1/150]$ nm^{-1} the corresponding curvature-induced DW velocity is expected to be about 80 m/s [49].

The curvature-induced dynamics are accompanied by the DW motion in the area of bigger curvature. In this way, in the energy (5) the last term becomes dominant. This term fixes the DW phase $\Phi = 0$ or $\Phi = \pi$, which depends on the sign of the product of the topological charge p and curvature $\kappa(q)$. Therefore, the transition to the precessional regime becomes suppressed. This effect can be interpreted as the curvature-induced suppression of the Walker limit. This is in contrast to the case of field-driven DWs in a straight wire, where the phase of the DW is not fixed (Zeeman term in the energy of DW is independent of the phase Φ [5,7]). Hence, a transition from translational to precessional regime of DW motion is possible.

Remarkably, the DW velocity (8) is similar to the well-known expression [50] $V^u = u\beta/\alpha$ in magnetic stripes with biaxial anisotropy caused by the Zhang-Li mechanism [9,10], where β is a nonadiabatic spin-transfer parameter. Current-induced translational DW motion takes place only if $u < u_{\mathrm{W}}$, where u_{W} is Walker current [15,50]. However, for the case of a geometry-induced motion, a Walker-limit-like effect of the transition to the precessional regime does not appear and the DW demonstrates a high-speed translational motion without any external driving. The DW behavior (8) is also similar to the dynamics of bubbles in a gradient magnetic field [5]. Still, in our case the DW moves in the direction of the gradient of the curvature, while bubbles are displaced in the perpendicular direction to the gradient of the field.

The DW velocity (8) is independent of the easy-plane anisotropy coefficient. However, this coefficient determines the time needed for the DW velocity to reach the asymptotic value (8). This time can be estimated as [42]

$$t_{\mathrm{as}} \approx -\frac{1 + \alpha^2}{\omega_0} \frac{\ln[(1 + \alpha^2)(1 - \varepsilon)]}{2\alpha k_p + \chi \ell^2}, \quad \varepsilon = \dot{q}/V, \quad (9)$$

where $\varepsilon < 1$ is the asymptotic parameter, which determines how close the instant velocity is to the asymptotic value (8). Additionally, the easy-plane anisotropy determines the maximal DW phase value $\Phi_{\max} = \Phi_0 + \varphi_{\max}$ with $\varphi_{\max} \approx -\mathcal{C} \pi \chi \ell^2 / (2\alpha k_p) \ll 1$ and $k_p > 0$. At long timescale, the
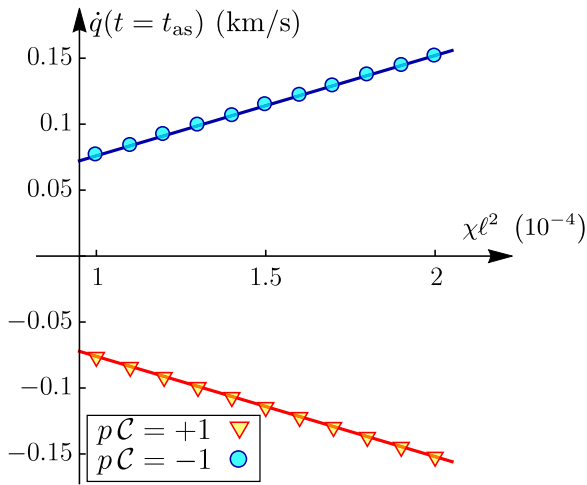
FIG. 4. DW velocity $\dot{q}$ as a function of the gradient of the curvature. Symbols show the instantaneous DW velocity at the moment t_{as} determined based on (9) for $\varepsilon = 0.9$. The data are obtained from NMAG micromagnetic simulations for the stripe with $w = 15$ nm, $h = 5$ nm, and $K_a = K_p = 0$ [42]. Solid lines show the dependence $\dot{q} = \varepsilon V$, where the asymptotic velocity V is determined based on Eq. (8).

change of the DW phase can be written as [42]

$$\Phi \approx \Phi_0 + p \frac{\Delta_0}{\alpha V t}, \qquad (10)$$

which results in the condition $\Phi(t \to \infty) = \Phi_0$. A typical time evolution of the DW position $q(t)$ and phase deviation $\varphi(t)$ is shown in Fig. 3.

In the no-damping approximation, the DW motion differs from (8) and (10). For the case of zero damping, the DW phase deviation reaches the value $\varphi(\alpha = 0) \to -\mathcal{C}\pi/2$, while the velocity of the DW increases exponentially with time within the considered model [42]. Note that for the velocities larger than the minimal phase velocity of magnons, the model should be revised by including the Cherenkov-like effect [27].

We checked the theoretically predicted velocities for the DW motion (8) by micromagnetic simulations of magnetically soft stripes with material parameters of Permalloy [51] using NMAG code [52] (see Figs. 3 and 4 and the Supplemental Material [42] for details). The numerics agrees well with the analytical prediction (8).

The resulting DW velocity as a function of the gradient of the curvature is plotted in Fig. 4. The DW velocity increases almost linearly with the gradient of the curvature. The direction of the DW motion depends on the sign of the product of the topological charge p, magnetochirality $\mathcal{C}$ of the DW, and sign of the gradient of the curvature χ ($\dot{q} \propto p\,\mathcal{C}\chi$)[see Figs. 3(a) and 4]. In Fig. 3(a) the DW position is shown as a function of time for walls with different sign of the product of the topological charge and magnetochirality: for $p\,\mathcal{C} = -1$, the DW moves in the direction of the increasing curvature. For the case $p\,\mathcal{C} = +1$, DW moves in the opposite direction (in both cases $\chi > 0$) [53].

In conclusion, we predict the effect of geometry-induced motion of a DW in a curved nanostripe: DWs are driven by the gradient of the stripe curvature without any external stimuli [see Eqs. (6) and (8)]. The physical origin of the driving force is the curvature-induced DMI driven by the exchange [32,33]. Geometry-induced motion results in a high-speed translational motion of the DW position without transition into the precessional regime. The latter effect can be interpreted as a curvature-induced suppression of the Walker limit. We show that the direction of the DW motion is determined by the product of the DW magnetochirality, topological charge, and gradient of the curvature $\dot{q} \propto p\,\mathcal{C}\chi$ [see Eq. (8)], while the change of the DW phase at long timescales results in $\Phi - \Phi_0 \propto 1/q(t)$. Additionally, it is necessary to mention that the coefficient of the easy-plane anisotropy determines the time (9), which is needed for the DW to reach the asymptotic velocity (8).

The linear model of the curvature-induced DW motion (6) can be used also for a three-dimensional wire with small torsion. The latter contributes to the negligibly small quadratic corrections. However, the role of the torsion becomes significant when the spin torques are applied [11].

[1] S. S. P. Parkin, M. Hayashi, and L. Thomas, Magnetic domain-wall racetrack memory, Science **320**, 190 (2008).

[2] P. Xu, K. Xia, C. Gu, L. Tang, H. Yang, and J. Li, An all-metallic logic gate based on current-driven domain wall motion, Nat. Nanotechnol. **3**, 97 (2008).

[3] A. Fert, V. Cros, and J. Sampaio, Skyrmions on the track, Nat. Nanotechnol. **8**, 152 (2013).

[4] S. Parkin and S.-H. Yang, Memory on the racetrack, Nat. Nanotechnol. **10**, 195 (2015).

[5] A. P. Malozemoff and J. C. Slonzewski, *Magnetic Domain Walls in Bubble Materials* (Academic, New York, 1979).

[6] A. Thiaville, J. M. Garcia, and J. Miltat, Domain wall dynamics in nanowires, J. Magn. Magn. Mater. **242-245**, 1061 (2002).

[7] *Spin Dynamics in Confined Magnetic Structures III*, Topics in Applied Physics Vol. 101, edited by B. Hillebrands and A. Thiaville (Springer, Berlin, 2006).

[8] J. C. Slonczewski, Current-driven excitation of magnetic multilayers, J. Magn. Magn. Mater. **159**, L1 (1996).

[9] Ya. B. Bazaliy, B. A. Jones, and S.-C. Zhang, Modification of the Landau-Lifshitz equation in the presence of a spin-polarized current in colossal- and giant-magnetoresistive materials, Phys. Rev. B **57**, R3213 (1998).

[10] S. Zhang and Z. Li, Roles of Nonequilibrium Conduction Electrons on the Magnetization Dynamics of Ferromagnets, Phys. Rev. Lett. **93**, 127204 (2004).

[11] K. V. Yershov, V. P. Kravchuk, D. D. Sheka, and Y. Gaididei, Curvature and torsion effects in spin-current driven domain wall motion, Phys. Rev. B **93**, 094418 (2016).

[12] R. Moreno, V. L. Carvalho-Santos, A. P. Espejo, D. Laroze, O. Chubykalo-Fesenko, and D. Altbir, Oscillatory behavior of the domain wall dynamics in a curved cylindrical magnetic nanowire, Phys. Rev. B **96**, 184401 (2017).

[13] N. L. Schryer and L. R. Walker, The motion of 180° domain walls in uniform dc magnetic fields, J. Appl. Phys. **45**, 5406 (1974).

[14] A. Thiaville and Y. Nakatani, Domain-wall dynamics in nanowires and nanostrips, in *Spin Dynamics in Confined Magnetic Structures III*, Topics in Applied Physics Vol. 101, edited by B. Hillebrands and A. Thiaville (Springer, Berlin, 2006), pp. 161–206.

[15] A. Mougin, M. Cormier, J. P. Adam, P. J. Metaxas, and J. Ferré, Domain wall mobility, stability and Walker breakdown in magnetic nanowires, Europhys. Lett. **78**, 57007 (2007).

[16] S.-H. Yang, K.-S. Ryu, and S. Parkin, Domain-wall velocities of up to 750 m s^{-1} driven by exchange-coupling torque in synthetic antiferromagnets, Nat. Nanotechnol. **10**, 221 (2015).

[17] Z. Meng, S. He, L. Huang, J. Qiu, T. Zhou, C. Panagopoulos, G. Han, and K.-L Teo, Current induced domain wall motion in anti-ferromagnetically coupled (Co$_{70}$Fe$_{30}$/Pd) multilayer nanowires, Appl. Phys. Lett. **109**, 142403 (2016).

[18] A. V. Khvalkovskiy, K. A. Zvezdin, Y. V. Gorbunov, V. Cros, J. Grollier, A. Fert, and A. K. Zvezdin, High Domain Wall Velocities Due to Spin Currents Perpendicular to the Plane, Phys. Rev. Lett. **102**, 067206 (2009).

[19] S. Emori, U. Bauer, S.-M. Ahn, E. Martinez, and G. S. D. Beach, Current-driven dynamics of chiral ferromagnetic domain walls, Nat. Mater. **12**, 611 (2013).

[20] K.-S. Ryu, L. Thomas, S.-H. Yang, and S. Parkin, Chiral spin torque at magnetic domain walls, Nat. Nanotechnol. **8**, 527 (2013).

[21] M. Yan, A. Kákay, S. Gliga, and R. Hertel, Beating the Walker Limit with Massless Domain Walls in Cylindrical Nanowires, Phys. Rev. Lett. **104**, 057201 (2010).

[22] P. Landeros and Á S. Núñez, Domain wall motion on magnetic nanotubes, J. Appl. Phys. **108**, 033917 (2010).

[23] J. A. Otálora, J. A. López-López, P. Vargas, and P. Landeros, Chirality switching and propagation control of a vortex domain wall in ferromagnetic nanotubes, Appl. Phys. Lett. **100**, 072407 (2012).

[24] J. A. Otálora, J. A. López-López, A. S. Núñez, and P. Landeros, Domain wall manipulation in magnetic nanotubes induced by electric current pulses, J. Phys.: Condens. Matter **24**, 436007 (2012).

[25] J. A. Otálora, J. A. López-López, P. Landeros, P. Vargas, and A. S. Núñez, Breaking of chiral symmetry in vortex domain wall propagation in ferromagnetic nanotubes, J. Magn. Magn. Mater. **341**, 86 (2013).

[26] R. Hertel, Ultrafast domain wall dynamics in magnetic nanotubes and nanowires, J. Phys.: Condens. Matter **28**, 483002 (2016).

[27] M. Yan, C. Andreas, A. Kákay, F. Garcia-Sanchez, and R. Hertel, Fast domain wall dynamics in magnetic nanotubes: Suppression of walker breakdown and Cherenkov-like spin wave emission, Appl. Phys. Lett. **99**, 122505 (2011).

[28] J.-Y. Chauleau, R. Weil, A. Thiaville, and J. Miltat, Magnetic domain walls displacement: Automotion versus spin-transfer torque, Phys. Rev. B **82**, 214414 (2010).

[29] D. E. Nikonov, S. Manipatruni, and I. A. Young, Automotion of domain walls for spintronic interconnects, J. Appl. Phys. **115**, 213902 (2014).

[30] K. Richter, A. Krone, Md.-A. Mawass, B. Krüger, M. Weigand, H. Stoll, G. Schütz, and M. Kläui, Localized domain wall nucleation dynamics in asymmetric ferromagnetic rings revealed by direct time-resolved magnetic imaging, Phys. Rev. B **94**, 024435 (2016).

[31] Md.-A. Mawass, K. Richter, A. Bisig, R. M. Reeve, B. Krüger, M. Weigand, H. Stoll, A. Krone, F. Kronast, G. Schütz, and M. Kläui, Switching by Domain-Wall Automotion in Asymmetric Ferromagnetic Rings, Phys. Rev. Appl. **7**, 044009 (2017).

[32] Y. Gaididei, V. P. Kravchuk, and D. D. Sheka, Curvature Effects in Thin Magnetic Shells, Phys. Rev. Lett. **112**, 257203 (2014).

[33] D. D. Sheka, V. P. Kravchuk, and Y Gaididei, Curvature effects in statics and dynamics of low dimensional magnets, J. Phys. A: Math. Theor. **48**, 125202 (2015).

[34] Anisotropy axis e_T in a curved magnet is spatially dependent, while e_B for planar wire is constant. Therefore, it is convenient to represent the energy of the magnet in the curvilinear Frenet-Serret reference frame with $e_T = \gamma'$ being a tangential (T), $e_N = \gamma''/|\gamma''|$ being a normal (N) and $e_B = e_T \times e_N$ being a binormal (B) vector, respectively (TNB basis).

[35] D. G. Porter and M. J. Donahue, Velocity of transverse domain wall motion along thin, narrow strips, J. Appl. Phys. **95**, 6729 (2004).

[36] A. Aharoni, Demagnetizing factors for rectangular ferromagnetic prisms, J. Appl. Phys. **83**, 3432 (1998).

[37] Y. B. Gaididei, A. Goussev, V. P. Kravchuk, O. V. Pylypovskyi, J. M. Robbins, D. Sheka, V. Slastikov, and S. Vasylkevych, Magnetization in narrow ribbons: Curvature effects, J. Phys. A: Math. Theor. **50**, 385401 (2017).

[38] V. P. Kravchuk, Stability of magnetic nanowires against spin-polarized current, Ukr. J. Phys. **59**, 1001 (2014).

[39] V. V. Slastikov and C. Sonnenberg, Reduced models for ferromagnetic nanowires, IMA J. Appl. Math. **77**, 220 (2012).

[40] J. C. Slonczewski, Dynamics of magnetic domain walls, Int. J. Magn. **2**, 85 (1972).

[41] K. V. Yershov, V. P. Kravchuk, D. D. Sheka, and Y. Gaididei, Curvature-induced domain wall pinning, Phys. Rev. B **92**, 104412 (2015).

[42] See Supplemental Material http://link.aps.org/supplemental/10.1103/PhysRevB.98.060409 for details of mathematical calculations and micromagnetic simulations, which includes Refs. [54–56].

[43] J. D. Lawrence, *A Catalog of Special Plane Curves (Dover Books on Mathematics)* (Dover, New York, 2014).

[44] We use the approximation of small DW phase in order to obtain an analytical estimation of the parameters of the DW motion. This estimation, in turn, is based on the numerical solutions of

Eqs. (6), which results in small DW phase even for a very large DW velocity.

[45] J.-S. Kim, Md.-A. Mawass, A. Bisig, B. Krüger, R. M. Reeve, T. Schulz, F. Büttner, J. Yoon, C.-Y. You, M. Weigand, H. Stoll, G. Schütz, H. J. M. Swagten, B. Koopmans, S. Eisebitt, and M. Kläui, Synchronous precessional motion of multiple domain walls in a ferromagnetic nanowire by perpendicular field pulses, Nat. Commun. **5**, 3429 (2014).

[46] E. R. Lewis, D. Petit, L. Thevenard, A. V. Jausovec, L. O'Brien, D. E. Read, and R. P. Cowburn, Magnetic domain wall pinning by a curved conduit, Appl. Phys. Lett. **95**, 152505 (2009).

[47] G. Nahrwold, L. Bocklage, J. M. Scholtyssek, T. Matsuyama, B. Krüger, U. Merkt, and G. Meier, Current-induced domain-wall depinning in curved permalloy nanowires, J. Appl. Phys. **105**, 07D511 (2009).

[48] A. Wartelle, J. Pablo-Navarro, M. Staňo, S. Bochmann, S. Pairis, M. Rioult, C. Thirion, R. Belkhou, J. M. de Teresa, C. Magén, and O. Fruchart, Transmission XMCD-PEEM imaging of an engineered vertical FEBID cobalt nanowire with a domain wall, Nanotechnology **29**, 045704 (2018).

[49] Calculations are performed for the curved stripe [46] with the material parameters of Permalloy [51] with thickness $h = 10$ nm and width $w = 100$ nm, which results in the DW width $\Delta_0 \approx 21.5$ nm. The dimensionless gradient of the curvature is calculated as $\chi \ell^2 = \ell^2 \kappa / L \approx 2 \times 10^{-4}$, where $L = 800$ nm is a length of a curved segment. The corresponding curvature-induced DW velocity (8) is expected to be $V \approx 82$ m/s.

[50] A. Thiaville, Y. Nakatani, J. Miltat, and Y. Suzuki, Micromagnetic understanding of current-driven domain wall motion in patterned nanowires, Europhys. Lett. **69**, 990 (2005).

[51] Material parameters are the following: exchange constant $A = 26$ pJ/m, saturation magnetization $M_s = 860$ kA/m, and damping coefficient $\alpha = 0.01$. These parameters result in the exchange length $\ell \approx 5.3$ nm and $\omega_0/(2\pi) \approx 30.3$ GHz. Thermal effects and anisotropy are neglected. In numerical simulations only two magnetic interactions were taken into account, namely, exchange and magnetostatic contributions.

[52] T. Fischbacher, M. Franchin, G. Bordignon, and H. Fangohr, A systematic approach to multiphysics extensions of finite-element-based micromagnetic simulations: Nmag, IEEE Trans. Magn. **43**, 2896 (2007).

[53] One has to notice a one-to-one correspondence between natural parameter s and gradient of the curvature χ with DW magnitochirality $\mathcal{C}$: change of the natural parameter sign results in the changing of gradient of the curvature and DW magnitochirality signs, therefore direction of DW motion physically is the same.

[54] W. Döring, Über die trägheit der wände zwischen weißchen bezirken, Z. Naturfors., A **3**, 373 (1948).

[55] T. L. Gilbert, A phenomenological theory of damping in ferromagnetic materials, IEEE Trans. Magn. **40**, 3443 (2004).

[56] *NIST Handbook of Mathematical Functions*, edited by F. W. J. Olver, D. W. Lozier, R. F. Boisvert, and C. W. Clark (Cambridge University Press, New York, 2010).